Supporting information

Synthesis of Hollow Biomineralized $CaCO_3$-Polydopamine Nanoparticles for Multimodal Imaging-Guided Cancer Photodynamic Therapy with Reduced Skin Photosensitivity

Ziliang Dong[†], Liangzhu Feng[†]*, Yu Hao[†], Muchao Chen[†], Min Gao[†], Yu Chao[†], He Zhao[‡], Wenwen Zhu[†], Jingjing Liu[†], Chao Liang[†], Qiao Zhang[†], Zhuang Liu[†]*

[†] Institute of Functional Nano & Soft Materials (FUNSOM), Jiangsu Key Laboratory for Carbon-Based Functional Materials & Devices, Soochow University, 199 Ren'ai Road, Suzhou, 215123, Jiangsu, PR China.

[‡] Department of Radiology, Children's Hospital of Soochow University, Suzhou 215003, Jiangsu, PR China.

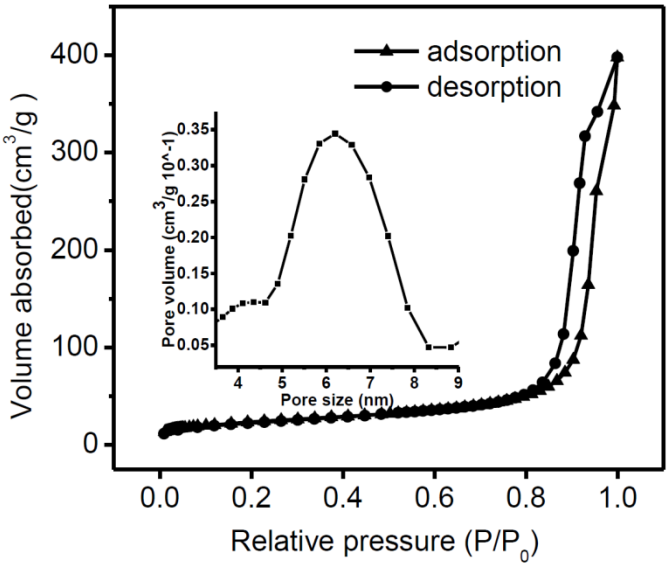

Figure S1. Nitrogen adsorption/desorption isotherms and the corresponding pore-size distribution curve (inset) of the $CaCO_3$-PDA sample.

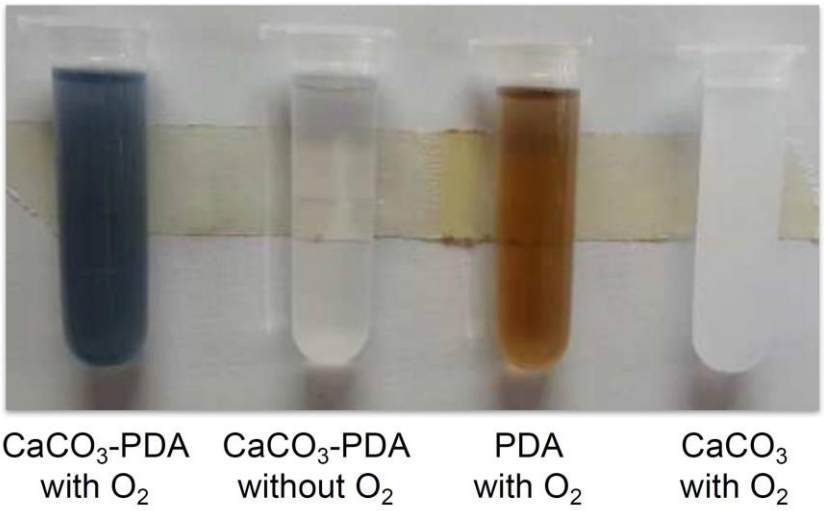

Figure S2. Digital photographs of $CaCO_3$-PDA nanoparticles grown in the presence or absence of oxygen, as well as $CaCO_3$ and PDA nanoparticles grown in the presence of oxygen.

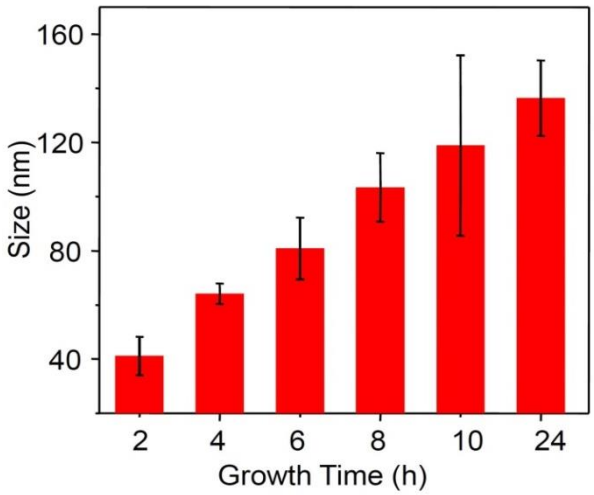

Figure S3. The time dependent particle size increases based on the TEM imaging of samples collected at different reaction time. .

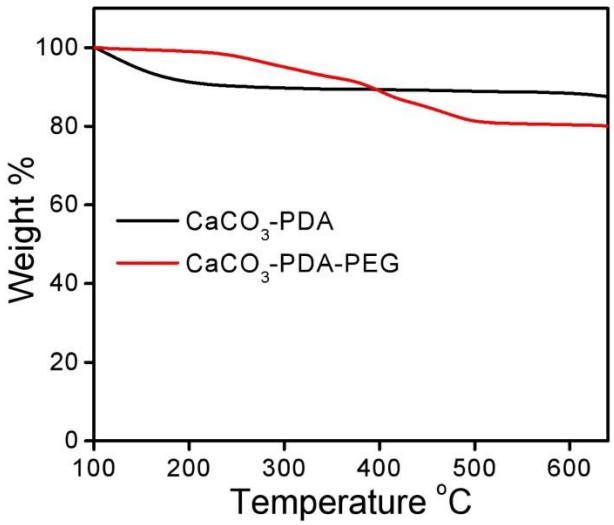

Figure S4. Thermogravimetric analysis curves of $CaCO_3$-PDA and $CaCO_3$-PDA-PEG hollow nanoparticles.

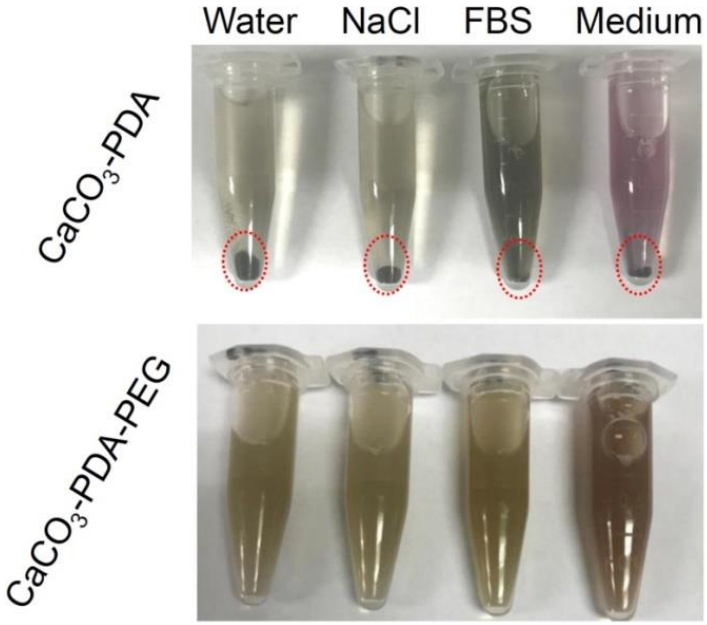

Figure S5. Digital photographs of $CaCO_3$-PDA and $CaCO_3$-PDA-PEG hollow nanoparticles in various solutions. Those nanoparticles showed excellent colloidal stability after PEGylation.

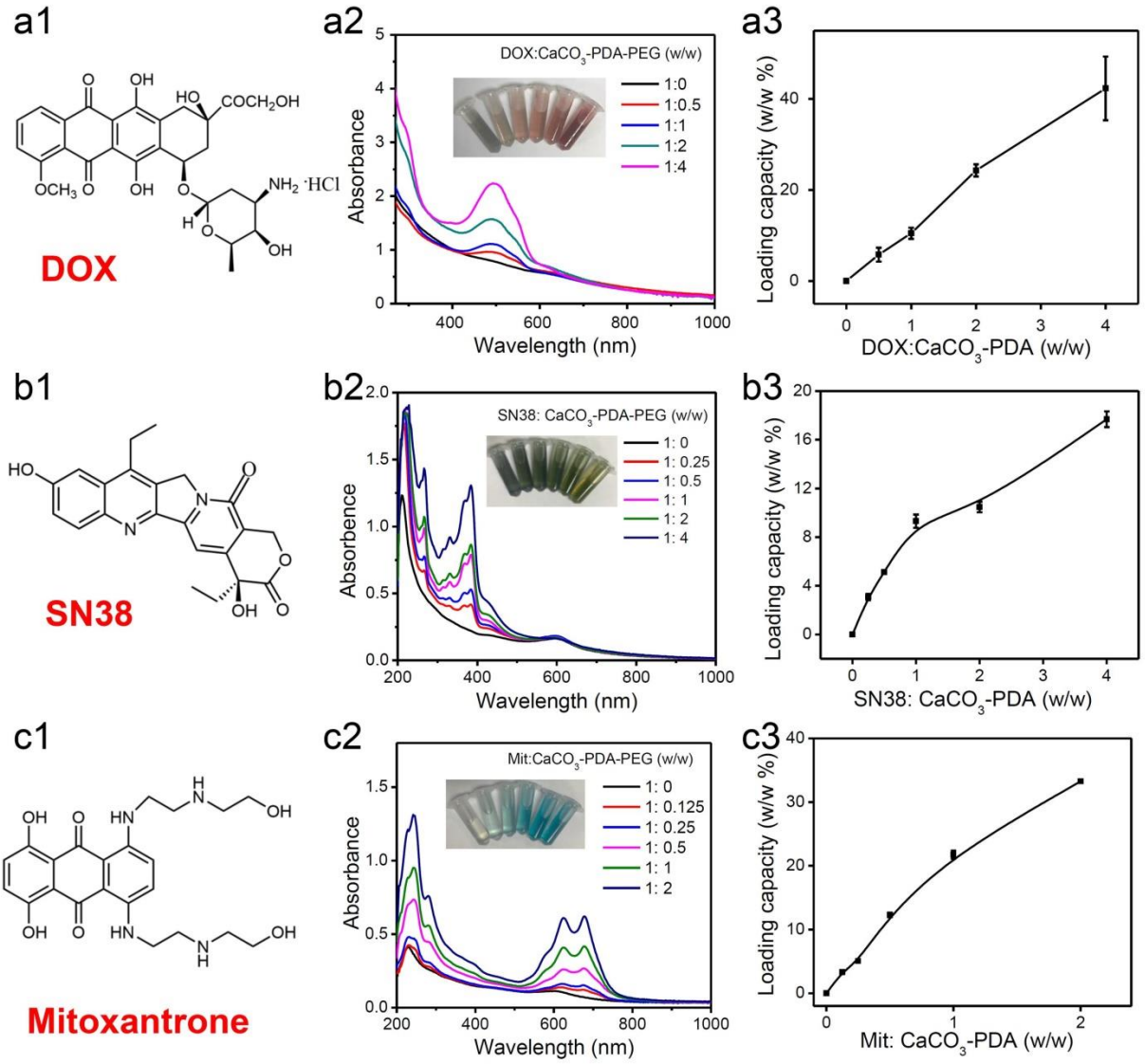

Figure S6. Drug loading capacities of $CaCO_3$-PDA. (a1, a2, a3) molecular structures of DOX (a1), SN38 (a2) and Mitoxantrone (a3). (b1, b2, b3)UV-Vis-NIR spectra of DOX (b1), SN38 (b2) and Mitoxantrone (b3) loaded $CaCO_3$-PDA at different feeding ratios of drug to $CaCO_3$-PDA. Inserted: photos of drug loaded $CaCO_3$-PDA. (c1, c2, c3) Quantification of DOX (c1), SN38 (c2) and Mitoxantrone (c3) loading capacities of $CaCO_3$-PDA at different drug: $CaCO_3$-PDA-PEG feeding ratios. In our experiments, drugs ((DOX, SN38 or mitoxantrone) at different weight ratios with $CaCO_3$-PDA was added to the $CaCO_3$-PDA (2 mg/mL) ethanol solutions under stirring overnight. Later, the free drugs were purified by repeatedly centrifuged with fresh ethanol solutions. The UV-Vis-NIR spectra was then used to quantitatively evaluate the drug loading capacity.

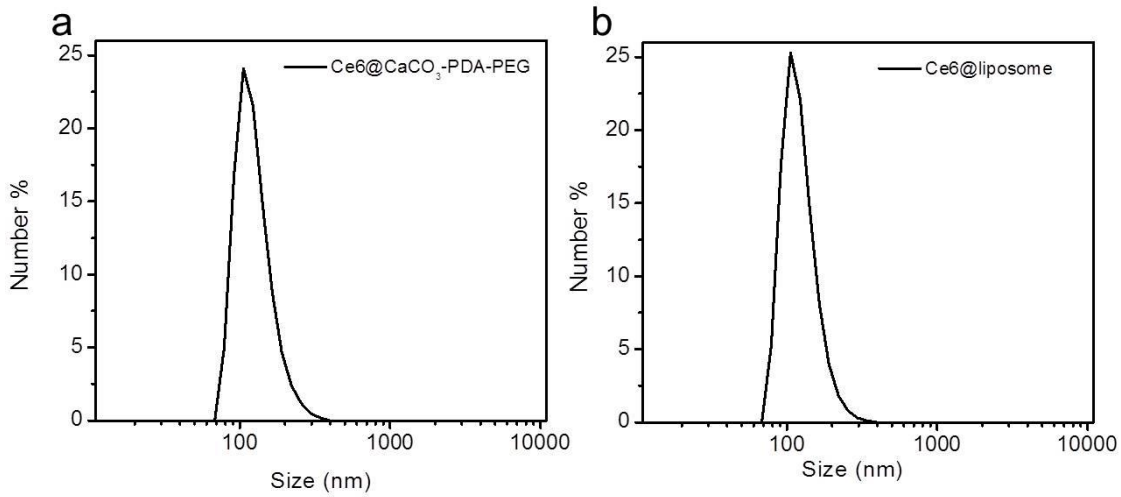

	Ce6@$CaCO_3$-PDA-PEG	Ce6@liposome
Size	173.6 nm	166.3 nm
PDI	0.232	0.226

Figure S7. Dynamic light scattering (DLS) data of Ce6@$CaCO_3$-PDA-PEG (a) and Ce6@liposome (b) and their corresponding particle dispersion index (PDI) in the aqueous solution.

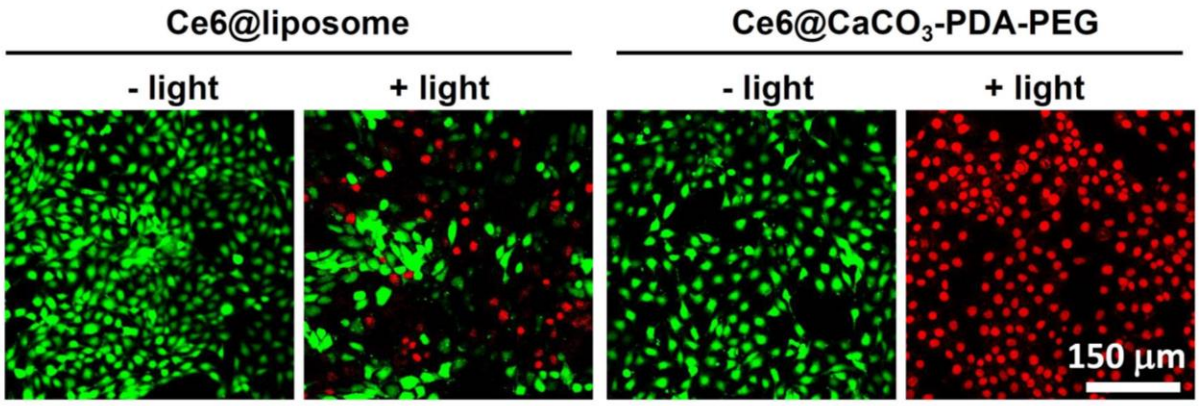

Figure S8. Confocal images of calcein AM (green: live cells) and propidium iodide (red: dead cells) co-stained 4T1 cells with different treatment.

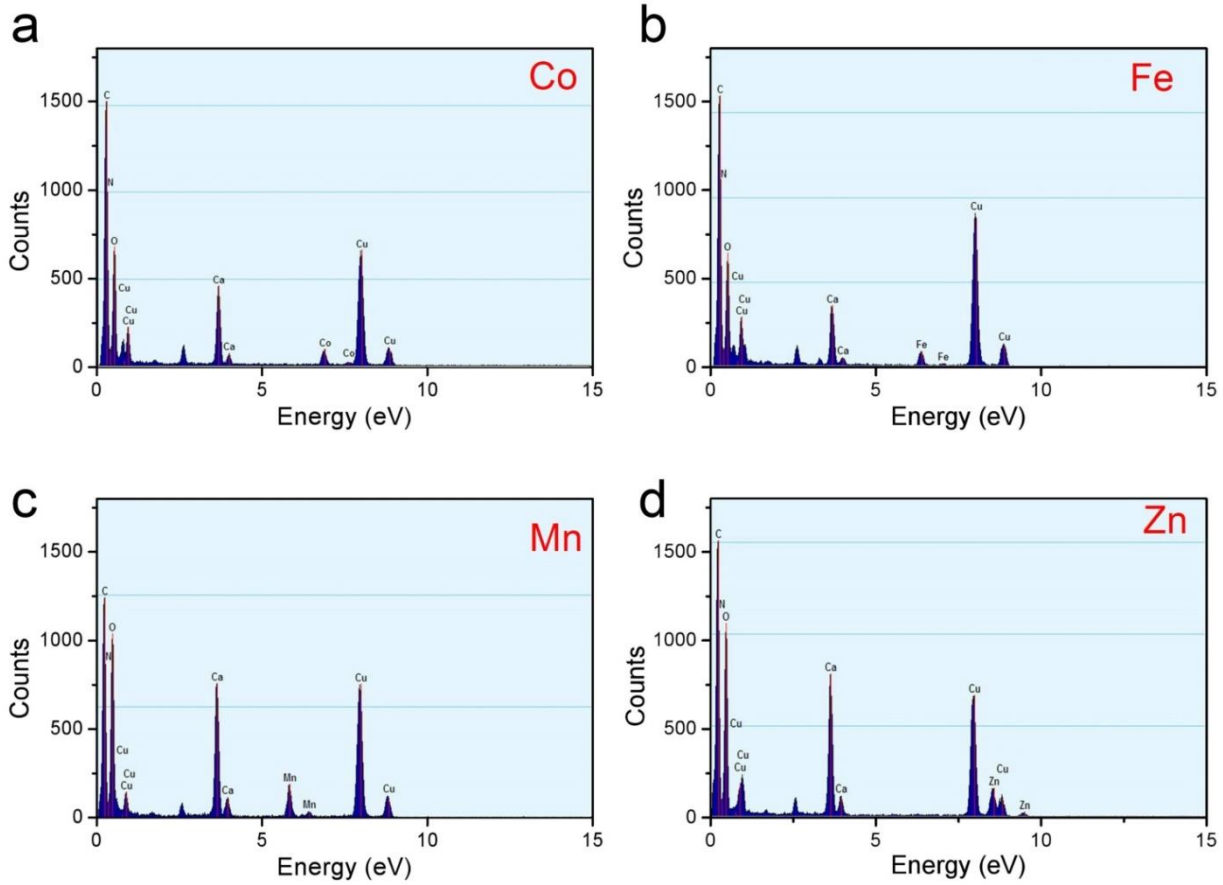

Figure S9. EDX spectra of Fe^{3+}, Zn^{2+}, Mn^{2+} and Co^{2+} doped $CaCO_3$-PDA hollow nanoparticles.

Ions \ Agents	$CaCO_3$-PDA	$CaCO_3$
Zn	0.34	0.3
Fe	4.08	0.82
Co	2.93	1.42
Mn	1.37	0.43

Table S1. Metal ions chelation capacities (Zn, Fe, Co or Mn) of $CaCO_3$-PDA hollow nanoparticles and bare $CaCO_3$ nanoparticles based on the quantitative energy dispersive spectrometer (EDS) analysis.

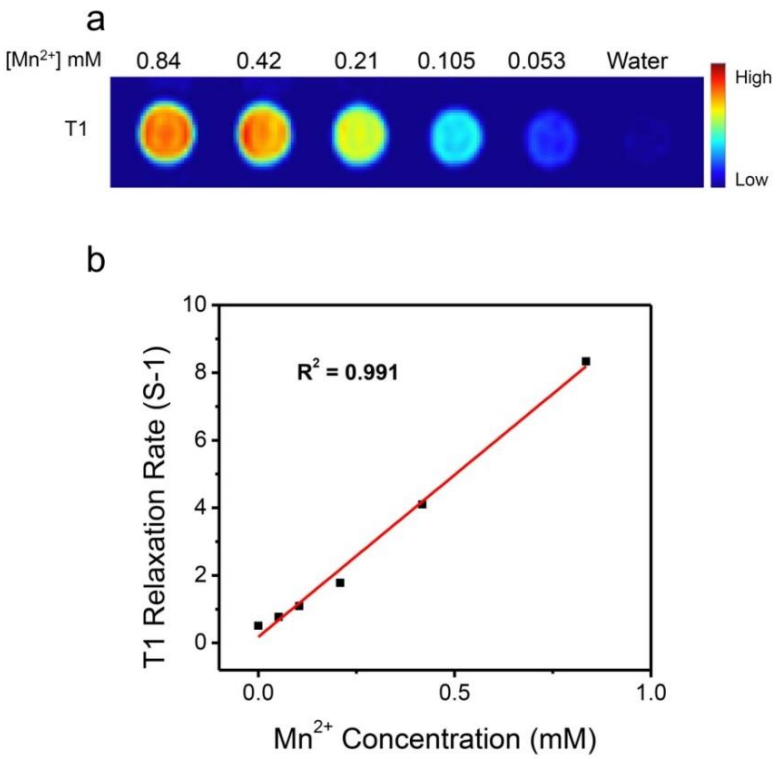

Figure S10. (a) T1 weighted MR imaging of $CaCO_3$-PDA(Mn)-PEG at various Mn^{2+} concentrations. (b) The T1 relaxation rates of $CaCO_3$-PDA(Mn)-PEG. The longitudinal relaxivity (r1) of $CaCO_3$-PDA(Mn)-PEG was determined to be 9.5 mM^{-1} s^{-1}.

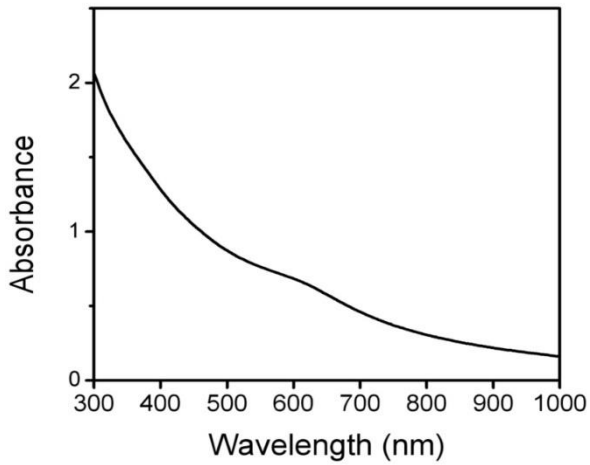

Figure S11. UV-Vis-NIR spectra of $CaCO_3$-PDA-PEG nanoparticles.

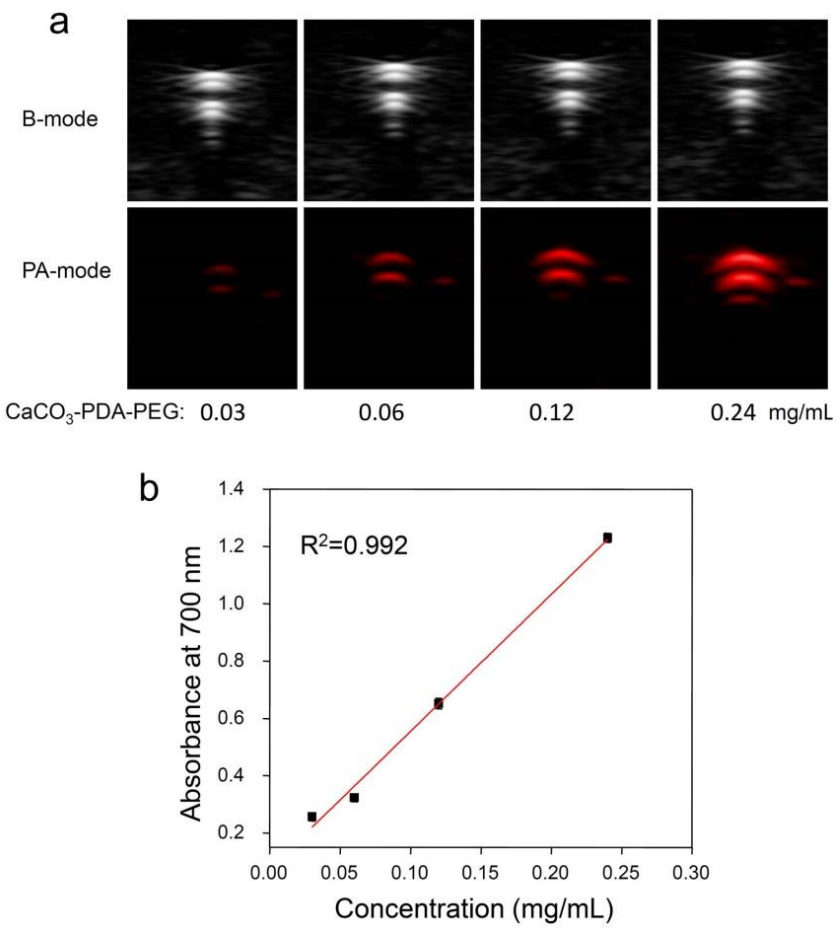

Figure S12. (a) PA imaging of $CaCO_3$-PDA-PEG at different concentrations under the Visualsonic Vevo® 2100 LAZER system (700 nm, 21 MHz). (b) Linear correlation of PA signal intensities of $CaCO_3$-PDA-PEG at 700 nm against its corresponding PDA concentrations.

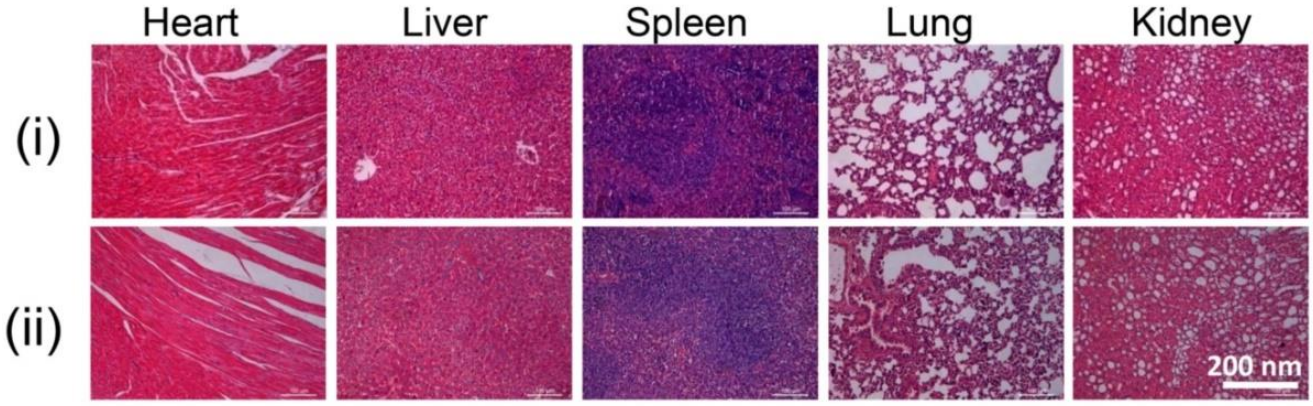

Figure S13. H&E staining of major organs collected from mice of different groups post treatments. No noticeable signs of organ damage appeared in all major organs of mice. Group (i) & (ii) were used to represent the group of mice treated with PBS injection only and Ce6@$CaCO_3$-PDA-PEG + Light exposure, respectively.

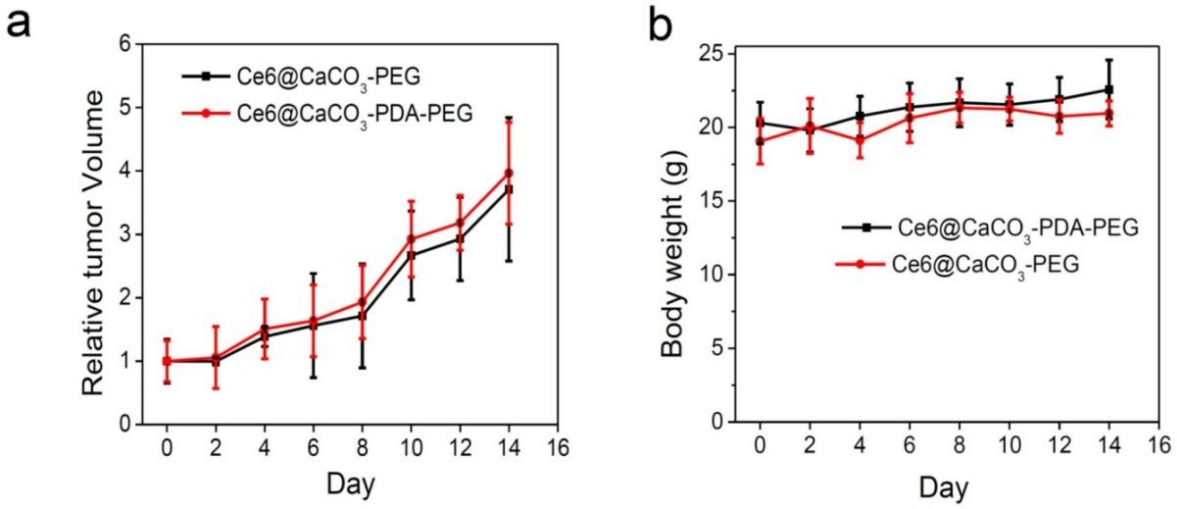

Figure S14. (a) Tumor growth curves of mice with i.v. injection of Ce6@$CaCO_3$-PEG or Ce6@$CaCO_3$-PDA-PEG and irradiated with 660 nm LED light at a power density of 5 mW cm^{-2} for 1 h, at 24 h post injection (5 mice for each group). (b) The body weight variation curves of the two groups of mice post different treatments.